# Residual biomass of gooseberry (*Ribes uva-crispa* L.) for the bioremoval process of Fe(III) ions

Tomasz Kalak[a,*], Joanna Dudczak-Hałabuda[a], Yu Tachibana[b], Ryszard Cierpiszewski[a]

[a]*Department of Industrial Products and Packaging Quality, Institute of Quality Science, Poznań University of Economics and Business, Niepodległości 10, 61-875 Poznań, Poland, Tel. +48 618569059; email: tomasz.kalak@ue.poznan.pl (T. Kalak), Tel. + 48 618569382; email: joanna.dudczak@ue.poznan.pl (J. Dudczak-Hałabuda), Tel. + 48 618569027; email: ryszard.cierpiszewski@ue.poznan.pl (R. Cierpiszewski)*
[b]*Department of Nuclear System Safety Engineering, Graduate School of Engineering, Nagaoka University of Technology, 1603-1, Kamitomioka, Nagaoka, Niigata 940-2188, Japan, Tel. +81 0258479570; email: yu_tachibana@vos.nagaokaut.ac.jp (Y. Tachibana)*

## ABSTRACT

Gooseberry (*Ribes uva-crispa* L.) residues were generated in processing in the food industry and taken for testing for the removal of Fe(III) ions from water in batch experiments. The biosorbent material was characterized using several analytical methods, including particle size distribution, X-ray diffraction analysis, elemental composition (scanning electron microscopy-energy dispersive X-ray spectroscopy), specific surface area, and average pore diameter (Brunauer–Emmett–Teller adsorption isotherms), volume of pores, and pore volume distribution (Barrett–Joyner–Halenda), thermogravimetry (TGA, DTG), morphology (scanning electron microscopy), Fourier transform infrared analysis. Several factors, such as adsorbent dosage, initial concentration, pH, and contact time were analyzed to show an effect on the biosorption process efficiency. The maximum adsorption efficiency was determined to be 88.5%. Based on the kinetics analysis, the bioremoval process is better described by the pseudo-second-order equation and the Langmuir model. In conclusion, gooseberry biomass can be an effective material for the efficient removal of iron(III) from wastewater and improving water quality.

*Keywords:* Water quality; Bioremoval process; Gooseberry residues; Fe(III) ions

## 1. Introduction

Water accounts for about 71% of the Earth's surface and plays the most important role in maintaining life. Moreover, freshwater only accounts for 3% of the total and is used for human consumption. Most of the freshwater is transferred for agricultural purposes, hence its unavailability and sometimes lack in many places is a significant social and economic problem [1]. Although access to clean drinking water has been improving in recent years, several million deaths a year worldwide are due to the consumption of contaminated water or drought. In the interests of environmental protection and the human population, new

and cheap technologies should be developed to purify water from pollution, which is a huge challenge for modern civilization [2].

Pollution of the environment, including oceans, seas, lakes, rivers, is mainly caused by the progressing development of the industry. Among many types of contaminants, heavy metals are considered the most dangerous because of their toxic properties. In addition, metals are not biodegradable nor capable of bioaccumulation and even at low concentrations (ppb) they are the cause of various diseases and disorders which may lead to fatal effects. Nowadays, they are removed from wastewater from various industries by means of many conventional but also expensive methods. An alternative seems to be the biosorption process, which is a much cheaper method and can use different types of

* Corresponding author.

biomass that are waste produced in industrial processing [3]. An example of biomass that can be used to bind heavy metal ions is gooseberry pomace generated in the food industry. In 2017, the global value of gooseberry production was estimated at around 169,369 tons and the greatest producer was Germany (86,480 tons). The next countries were listed as follows: Russia (58,551 tons), Poland (9,457 tons), Ukraine (7,820 tons), and the United Kingdom (2,538 tons). Production in Poland ranges on average between 14 and 20 thousand tons/y and the area harvested oscillates around between 2 and 3 thousand ha [4]. Several products, such as jams, marmalades, juices, powders, sauces, wines, liqueurs, and others are made from gooseberry fruit. It is rich in beneficial elements to human health, such as proteins, lipids, anthocyanins (cyanidin-3-glycosides, cyanidin-3-rutinosides), carbohydrates, fiber, vitamins A, B1, B2, B3, B6, B12, C, minerals, and pectins [5]. In addition, volatile constituents, such as C6-compounds ((Z)-hex-3-enal, (E)-hex-2-enal, (Z)-hex-3-en-1-ol, (E)-hex-2-en-1-ol, (E)-hex-3-enal) and esters (methyl butanoate, ethyl butanoate, methyl (E)-but-2-enoate, ethyl (E)-but-2-enoate, methyl hexanoate) are reported in its composition [6]. These substances contain functional groups (hydroxyl, carboxyl, phenolic, sulfo, and amino groups) that are capable of binding metal ions. The binding mechanism can take place by means of ion exchange, complexation, and chelation reactions. Furthermore, physical adsorption, redox reactions, or microprecipitation may occur. This process can also involve all of these reaction mechanisms simultaneously [7].

The purpose of the studies was to determine the physicochemical properties of gooseberry (*Ribes uva-crispa* L.) pomace generated from the processing in the food industry. In addition, the aim was to study the efficiency of bioremoval of Fe(III) ions from aqueous solutions by the biomass under different conditions of adsorbent dosage, initial concentration, pH, and contact time. Moreover, the biosorption kinetics, equilibrium, and the Langmuir and Freundlich isotherms were analyzed.

## 2. Experimental procedure

### 2.1. Materials and methods

#### 2.1.1. Gooseberry preparation

Gooseberry (*Ribes uva-crispa* L.) residues were generated during processing of the food industry in Poland. The biomass was crumbled, sieved, and separated into individual fractions. Afterwards, it was dried at a temperature of 60°C and stored in a desiccator prior to all experiments. Triplicate measurements were conducted and distilled water was used.

#### 2.1.2. Gooseberry residues characterization

The gooseberry particles with diameters ranging from 0 to 0.212 mm were used in the studies. In the first stage physicochemical properties of the biomaterial were analyzed using a variety of analytical methods, including: (1) particle size distribution analyzed by the laser diffraction method using a Zetasizer Nano ZS (Malvern Instruments Ltd., UK); (2) the elemental composition and mapping using a scanning electron microscopy (SEM) Hitachi S-3700N (Krefeld, Germany) with an attached a Noran SIX energy dispersive X-ray spectrometer (EDS) microanalyzer (ultra-dry silicon drift type with resolution (FWHM) 129 eV, accelerating voltage: 20.0 kV); (3) thermogravimetry analyzed by setsup DTG (first derivative of thermal gravimetric analysis), DTA (first derivative of temperature for thermal phase transitions) Setsys 1200 (Setaram, Caluire, France; temperature range 30°C–600°C; the rate of temperature increase 10°C/min; gas flow rate of nitrogen 20 mL/min); (4) the specific surface area and the average pore diameter by the Brunauer–Emmett–Teller (BET) method using Autosorb iQ Station 2 (Quantachrome Instruments, USA); (5) the pore volume by the Barrett–Joyner–Halenda (BJH) method using Autosorb iQ Station 2 (Quantachrome Instruments, USA); (6) the morphology by a SEM EVO-40 (Carl Zeiss, Germany); (7) the surface structure analysis by a Fourier transform attenuated total reflection (FT-IR ATR) spectrum 100 (Perkin-Elmer, Waltham, USA).

#### 2.1.3. Fe(III) biosorption process

Biosorption efficiency of Fe(III) ions on gooseberry residues were examined in batch experiments at room temperature ($T = 23°C \pm 1°C$). For this purpose, Fe(III) ions with analytical purity (standard for AAS 1 g/L, Sigma-Aldrich (Germany)) were used. The dried particles of gooseberry residues (2.5–100 g/L) and a portion of Fe(III) solution ranging from 2.5 to 20 mg/L at selected pH (2–5) were shaken at 150 rpm during 60 minutes. The pH of Fe(III) solutions was adjusted using 0.1 M NaOH and HCl. Afterwards, the solutions were centrifuged at 4,000 rpm to separate the phases. In the final stage, after the biosorption processes the Fe(III) ions concentration (mg/L) was determined by the atomic absorption spectrophotometer (F-AAS, at a wavelength $\lambda = 248.3$ nm for iron) SpectrAA 800 (Varian, Palo Alto, USA). The triplicate measurements were conducted and average results were presented.

The biosorption efficiency $A$ (%) and capacity $q_e$ (mg/g) were calculated according to the Eqs. (1) and (2), respectively:

$$A = \left[ \frac{C_0 - C_e}{C_0} \right] \times 100\% \tag{1}$$

$$q_e = \frac{(C_0 - C_e) \times V}{m} \tag{2}$$

where $C_0$ and $C_e$ (mg/L) are initial and equilibrium Fe(III) ion concentrations, respectively; $V$ (L) is the volume of solution and $m$ (g) is the mass of a biosorbent.

Kinetic and isotherm parameters were calculated using pseudo-first-order (Eq. (3)) and pseudo-second-order (Eq. (4)), Langmuir (Eq. (5)), and Freundlich (Eq. (6)) models in accordance with the equations, respectively:

$$q_t = q_e \left( 1 - e^{k_1 t} \right) \tag{3}$$

$$q_t = \frac{q_e^2 k_2 t}{1 + q_e k_2 t} \tag{4}$$

$$q_e = \frac{q_{\max} K_L C_e}{1 + K_L C_e} \tag{5}$$

$$q_e = K_F C_e^{\frac{1}{n}} \tag{6}$$

where $q_t$ (mg/g) is the amount of Fe(III) ions adsorbed at any time $t$ (min); $q_e$ (mg/g) is the maximum amount of Fe(III) ions adsorbed per mass of the biosorbent at equilibrium; $k_1$ (1/min) is the rate constant of pseudo-first-order adsorption; $k_2$ (g/(mg min)) is the rate constant of pseudo-second-order adsorption; $q_{\max}$ (mg/g) is the maximum adsorption capacity; $K_L$ is the Langmuir constant; $C_e$ (mg/L) is the equilibrium concentration after the adsorption process; $K_F$ is the Freundlich constant and $1/n$ is the intensity of adsorption.

## 3. Results and discussion

### 3.1. Characterization of the adsorbent

The particle size distribution has an influence on various properties of materials in the form of powder, granules, suspension, emulsion, or aerosol, including speed and strength of hydration. In addition, it is an important indicator of the quality and efficiency of particles in various processes. It is characteristic that smaller particles have the ability to dissolve faster and achieve better suspension than larger ones. Suspensions and emulsions are more stable due to smaller droplet sizes and higher surface charge. Furthermore, smaller particle sizes of adsorbents result in higher efficiency of adsorption processes [8,9]. In these studies, the particle size distribution of gooseberry residues was determined by laser diffraction and one peak was indicated at 68.6 nm. It should be clarified that the analysis was limited to some extent, that is, not all gooseberry particles formed suspension in the solution (larger particles fell to the bottom of the solution). Thus, it was only possible to analyze the particles suspended.

For the elemental analysis of samples, the scanning electron microscopy-energy dispersive X-ray spectroscopy (SEM-EDS) method was used, and the results are shown in Fig. 1 and Table 1. The peaks present in the spectrum correspond to the following elements, from the largest amount to the smallest (by weight (%)): O, C, Si, Al, Fe, K, Na, Mg, Ca, P, and Ti. Gooseberry is organic biomass, thus during the analysis the presence of the largest number of oxygen and carbon atoms was observed. The content of elements was not estimated on the bases of measurements but was calculated based on the number of counts in the EDS microanalysis. The gooseberry material is not homogeneous, so depending on the position of the measuring point on the sample using the SEM-EDS method, there may occur differences in the quantitative and qualitative composition.

The Fe(III) distribution on the biomass was determined by SEM-EDS mapping using the backscattered detector. The analysis of elements C, O, Ca, Al, P, Si, S, and K indicated a low deviation of their ratio in the observed area (Fig. 2). Almost homogeneous distribution was observed, however, the intensity depends on the kind of the particular element. It is observed in the images for carbon, oxygen, and calcium that the elements are able to form close clusters, which are visible as places of brighter colors on the surface of the samples.

The thermogravimetric measurements ranging from 29°C to 600°C were carried out. The results showed that there is a decrease in the material mass with the rise of temperature. Two steps of gooseberry decomposition are reported. The first one occurs between about 30°C and 110°C and the other in the range between 160°C and 470°C. A slight

Table 1
Average elements composition of gooseberry (determined by EDS microanalyzer)

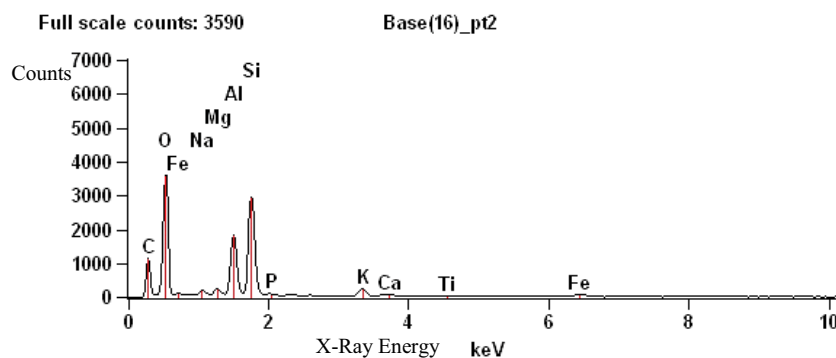| Elements | Weight (%) | Atomic (%) |
|---|---|---|
| C | 19.3 | 27.28 |
| O | 53.59 | 56.86 |
| Na | 0.85 | 0.63 |
| Mg | 0.78 | 0.55 |
| Al | 7.58 | 4.77 |
| Si | 13.85 | 8.37 |
| P | 0.29 | 0.16 |
| K | 1.36 | 0.59 |
| Ca | 0.5 | 0.21 |
| Ti | 0.14 | 0.05 |
| Fe | 1.76 | 0.54 |



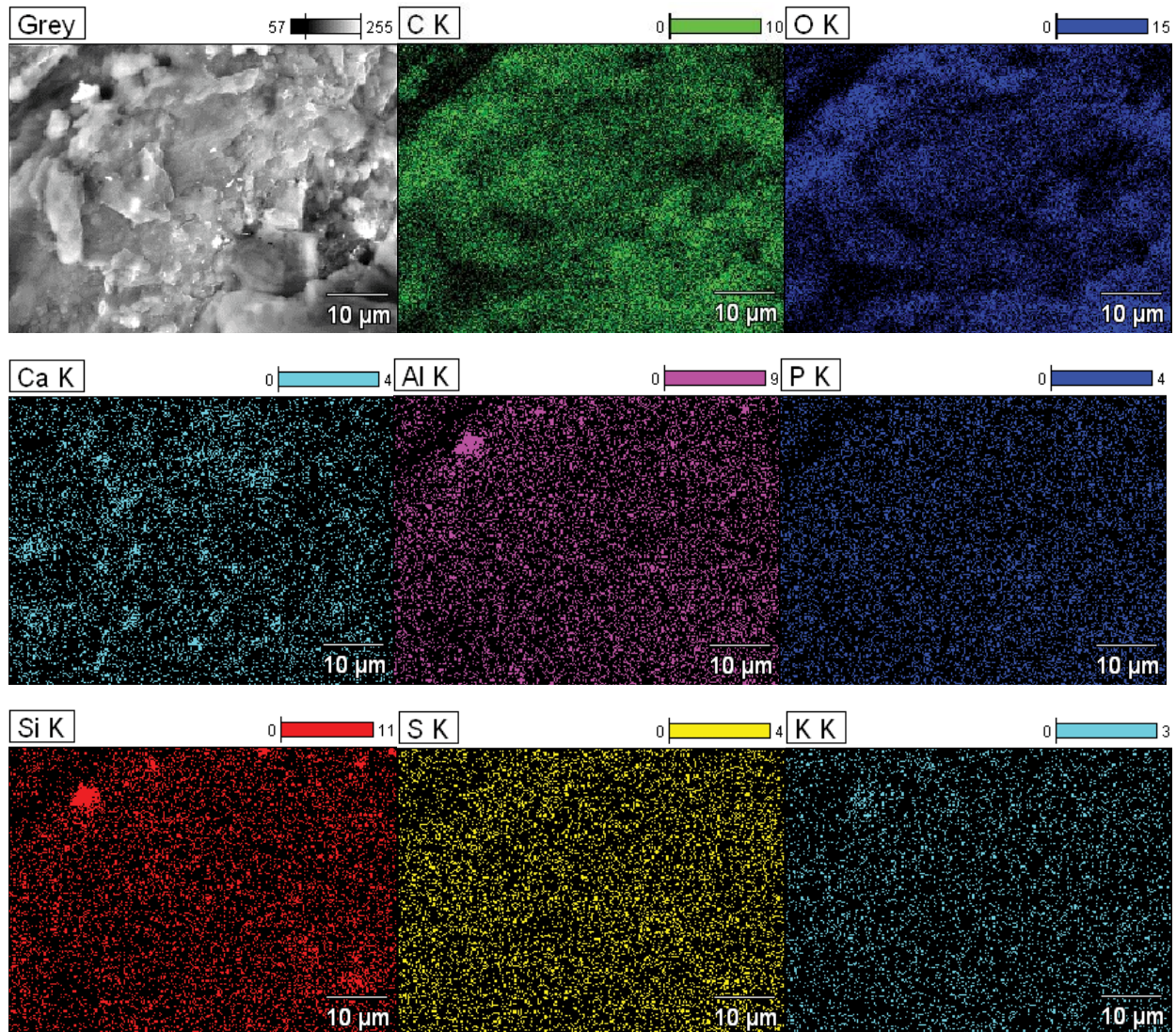Fig. 1. EDS spectrum of gooseberry residues.

Fig. 2. SEM-EDS images (mapping) of the distribution and relative proportion (intensity) of defined elements (C, O, Ca, Al, P, Si, S, and K) over the scanned area of gooseberry (magnification ×2,000).

weight loss (2.3%) is observed in the first stage probably as a result of the volatilization of adsorbed water molecules from the surface of the biosorbent sample. A greater mass loss (about 34.3%) is caused by the pyrolysis process in the subsequent stage, where most volatile substances are evaporated. The strong peak (DTG) in the temperature of 333°C corresponds to the decomposition of organic substances, such as carbohydrates, proteins, and lipids [10].

The BET analysis was performed and the parameters of the specific surface area ($S_{BET}$), volume of the pores ($V_p$), and average pore diameter ($A_{pd}$) are presented in Table 2. The adsorption and desorption isotherms fit into the type II adsorption behavior. The curve's intermediate flat surface refers to the formation of a monolayer. According to IUPAC (International Union of Pure and Applied Chemistry) nomenclature, the gooseberry contains pores with diameters between 2 and 50 nm, which classifies them as mesopores [11]. Pore volume distribution was determined by the BJH method, which relates to capillary condensation occurring in mesopores.

## 3.2. Biosorption of Fe(III) by the use of gooseberry

### 3.2.1. Effect of biosorbent dosage

The impact of gooseberry dosage on the removal of Fe(III) in the pH range 2–5 is shown in Fig. 3. The experiments were performed under the following conditions: initial concentration 10.7 mg/L, equilibrium pH 2.1–2.9, contact time 60 min, $T = 23$°C $\pm$ 1°C. As it is seen, the adsorption efficiency increased with the increase in the dosage up to 50–70 g/L. The dose of 70 g/L can be considered optimal, where the maximum removal efficiency is about 88.5% at pH 3. However, good results are also observed at pH 4, where high removal efficiency of 83%–84% was achieved at dosage of 10–20 g/L. Further increase in the adsorbent dose did not cause

significant changes and the adsorption remained at 84%. Moreover, the experimental adsorption capacity decreased from 2 to 0.1 mg/g. The phenomenon can be explained in the way that active centers are fully utilized during interaction between the biomass and iron ions at lower masses and are not fully utilized at greater ones [12]. The increase in process efficiency may be associated with the greater number of available binding sites for metal ions resulting from weight gain [13–15].

### 3.2.2. Effect of the initial concentration of Fe(III)

The influence of the initial concentration of Fe(III) ions on the bioremoval process was analyzed and the results are presented in Fig. 4. The experiments were carried out in the following conditions: initial concentration ranging from 2.5 to 20 mg/L, initial pH 4, contact time 60 min, $T = 23°C ± 1°C$, optimal gooseberry dosage 50 g/L. A sudden increase in the biosorption efficiency is observed after increasing initial concentration up to 2.5 mg/L. In the concentration range from 2.5 to 20 mg/L, only a slight increase in efficiency was noted from 95.5% to 98.5%. The equilibrium pH after adsorption ranged between 3.6 and 3.9. In the analyzed

biosorption process, the saturation of the gooseberry surface is dependent on the initial concentration of Fe(III)ions. At higher concentrations, iron ions can diffuse onto the gooseberry surface by means of intramolecular diffusion, while the process of diffusing hydrolyzed ions can take place much more slowly. At the initial stage of the process, the lower Fe(III) concentration was sufficient to initiate ion transfer between the aqueous and solid phases. The literature shows that the greater the driving force of mass transfer, the lower resistance to metal uptake and, as a result, the higher efficiency of metal ion removal [16]. According to literature, the $Fe^{3+}$ ionic radius is estimated at 65 pm [17]. Along with the smaller metal ionic radius, there is a

Table 2
Summary of BET adsorption and desorption parameters

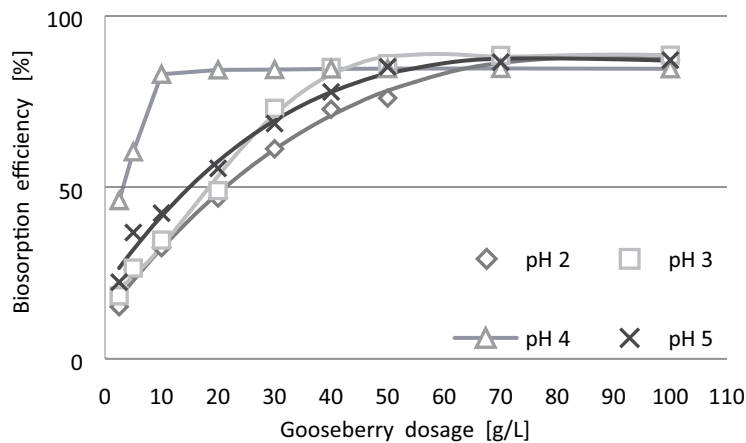| Parameters | Values |
| --- | --- |
| Specific surface area ($S_{BET}$) [m²/g] | 5.231 |
| Pore volume ($V_p$) [cm³/g] | 0.0045 |
| Pore diameter ($A_{pd}$) [nm] | 3.44 |



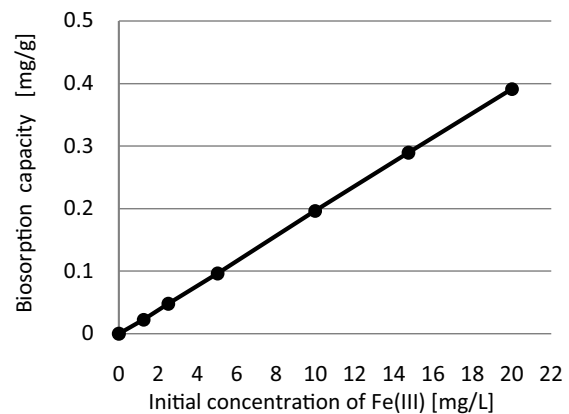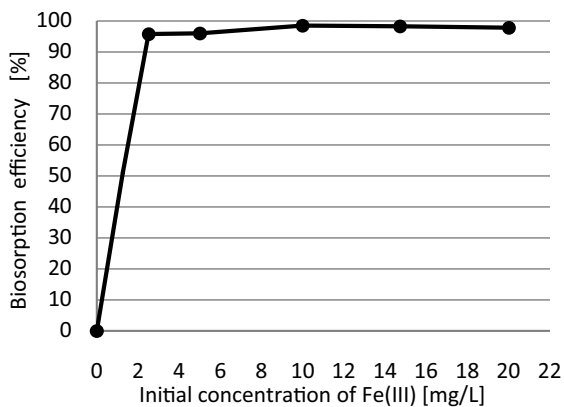Fig. 3. Effect of adsorbent dosage on biosorption efficiency of Fe(III) ions.



Fig. 4. (a and b) Effect of initial concentration on the Fe(III) biosorption efficiency (a) and capacity (b).

greater tendency to exhibit hydrolysis reactions resulting in a decrease in biosorption efficiency [18].

### 3.2.3. Impact of initial pH

The influence of initial pH on the bioremoval process was analyzed and the results are shown in Fig. 5. The experiments were conducted in the following conditions: initial concentration 10.7 mg/L, pH range 2–5, contact time 60 min, $T = 23°C ± 1°C$, gooseberry dosage 2.5–100 g/L. A strong dependence is seen between the biosorption efficiency, pH, and gooseberry dosage. Furthermore, the process is also dependent on values of interfacial tension and contact angle at the solid–liquid interface [19]. Fig. 5 shows that more favorable biosorption conditions and greater affinity for active sites caused an increase in the process efficiency. Maximum adsorption was obtained at pH 3 for dosage of 100 g/L ($A = 88.5\%$). Moreover, the achieved values were in the range between 87.1% and 88.5% at pH 2–5 (dosage 70–100 g/L), and no important changes were reported. The lowest biosorption was noticed at adsorbent dosage of 2.5 g/L ($A = 15.1\%$ at pH 2; $A = 22.3\%$ at pH 5). At pH 4 in the dosage range between 2.5 and 40 g/L a great increase in efficiency was noted. In general, it can be stated that under the applied experimental conditions, the higher gooseberry dosage, the greater process efficiency was observed. With high probability, iron ions are bound as a result of the cation exchange mechanism. Excess hydrogen ions protonated various functional groups present on the gooseberry surface and led to a decrease in the number of negatively charged sites. As the pH increased, acidic biosorbent groups were deprotonated and there was a chance to bind positively charged Fe(III) ions. Iron occurs in the ionic form at pH 2–5, hence the maximum sorption capacity was mainly achieved at pH 4. At pH above 4, a decrease in the process efficiency (in the range of biomass doses 2.5–40 mg/L) can be explained by the competition of hydroxyl ions in adsorption centers. In addition, the formation of other forms of iron compounds, including $Fe(OH)^{2+}$, $Fe(OH)_2^+$, and $Fe(OH)_3$ also has an effect on slowing down the biosorption process [15,20–23].

### 3.2.4. Kinetic studies on adsorption

#### 3.2.4.1. Impact of contact time

The results of the effect of contact time on the process are shown in Fig. 6. Based on the previous tests, the experimental conditions were set as follows: initial concentration 10 mg/L, gooseberry dosage 40 g/L, initial pH 4.0, $T = 23°C ± 1°C$. As it is seen in Fig. 6, the maximum sorption capacity was achieved during the first 5 min of the experiment (56.2%), and no significant changes were reported up to 300 minutes (55.6%–56.2%). The equilibrium pH was estimated at 4.52. The availability of more free active sites on the gooseberry surface and the high concentration of iron cations at the biosorbent-water interface may be the reason for this rapid initial increase in biosorption. At the time when active centers were occupied by Fe(III) cations, the biosorption equilibrium was achieved gradually, and the reaction mechanism could be different [24].

#### 3.2.4.2. Pseudo-first-order and pseudo-second-order kinetic models

Kinetics of Fe(III) biosorption on gooseberry was studied and the calculated parameters are presented in Table 3. The calculated correlation coefficient $R^2$ for the pseudo-first-order kinetic model is quite low, so pseudo-second-order model was analyzed in the next stage. As it is seen, the much higher calculated correlation coefficient suggests that the reaction process is better described by the pseudo-second-order model. In all likelihood, at the gooseberry surface, chemisorption reaction with Fe(III) ions occurred [25].

### 3.2.5. Adsorption isotherms

The Langmuir and Freundlich isotherm models were used in order to describe the bioremoval process. In accordance with the calculated data presented in Table 4, the isotherm parameters are better suited into the Langmuir equation model. The constant $K_L$ refers to the solute-binding
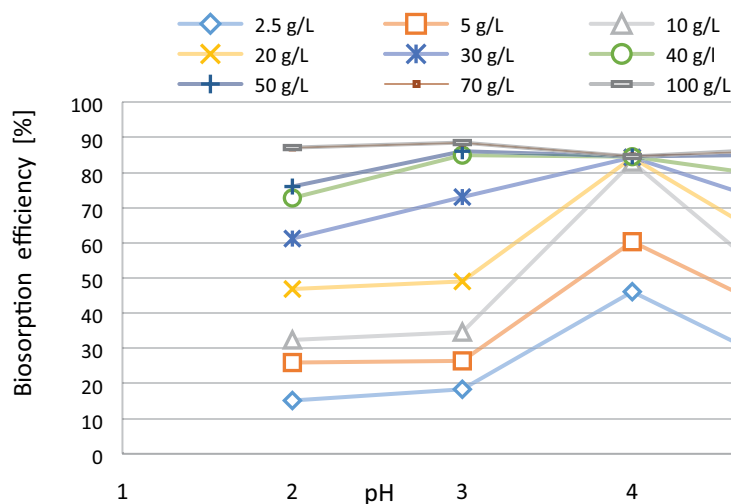


Fig. 5. Effect of pH on the Fe(III) biosorption efficiency at gooseberry dosage 2.5–100 g/L.
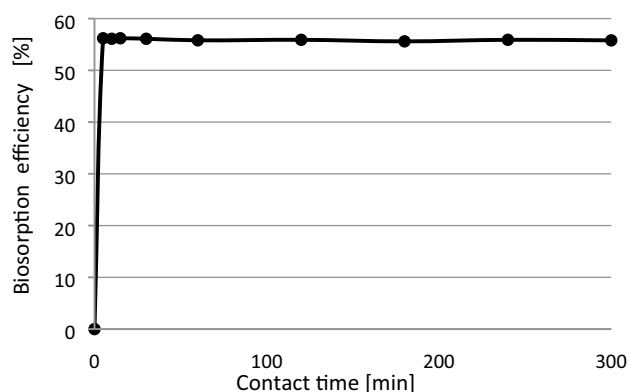
Fig. 6. Effect of contact time on the Fe(III) biosorption efficiency.

energy, the biosorbent and the spontaneity of the sorption process. It is assumed that the spontaneity increases with an increase in the $K_L$ value [26]. The Freundlich equation refers to the relationship between the concentration of metal ions at equilibrium ($C_e$) and the ions concentration per unit mass of an adsorbent ($q_e$) [27]. Based on the calculated Freundlich isotherm parameters, it can be said that the Fe(III) ions are able to bind from the solution. A comparison between the maximum adsorption capacity obtained in these studies and literature data is shown in Table 5.

### 3.3. Analysis of SEM images

SEM images of gooseberry before and after adsorption with iron were analyzed (Fig. 7). In general, irregular shape with many cavities is a typical characteristic feature of the biomass. Furthermore, when it comes to details, the particles are of various shapes: oval, short, and longitudinal, without sharp edges. The structure is not homogeneous and developed flat surfaces are visible. Moreover, greater particles characterize larger irregularities compared to smaller ones. After the iron ion biosorption process, it can be seen that the gooseberry surface has become rough, the small gaps have become filled and the agglomeration of particles has occurred. The surface appears more irregular with a large amount of small agglomerates attached to larger parts of the material. Texture changes visible in the images may likely be a confirmation of iron ion biosorption phenomena on the gooseberry surface.

### 3.4. FT-IR analysis

The FT-IR measurements of gooseberry before and after the biosorption process were conducted and the spectra are presented in Fig. 8. Based on the previous results, following conditions were chosen to the experiment: initial concentration 10.7 mg/L, initial pH 2.0, gooseberry dosage 100 g/L, $T = 23°C \pm 1°C$. The explanation of the FT-IR peaks is included in Table 6. Comparative analysis of gooseberry spectrum before and after Fe(III) biosorption was carried out taking into account differences in frequency, shape and intensity of the bands or possible interactions with iron ions. Fig. 8 shows that after the biosorption process the peak intensity shifted significantly toward lower transmittance values, and their positions remained at the same wavelengths or slightly shifted. The most important changes include: 3,289.5 (shift to 3,302.4 cm$^{-1}$), 2,922.8 (shift to 2,923.1 cm$^{-1}$), 2,853.9 (shift to 2,853.7 cm$^{-1}$), 1,739.9 (shift to 1,736 cm$^{-1}$), 1,624.1 (shift to 1,627.2 cm$^{-1}$), 1,517.3 (shift to 1,517.1 cm$^{-1}$), 1,033.1 (shift to 1,033 cm$^{-1}$), 455 (shift to 455.4 cm$^{-1}$), 419 (shift to 426.8 cm$^{-1}$), and 392.7 (shift to 396.1 cm$^{-1}$). The observed phenomena may result from the chemisorption process due to the interaction of iron ions with functional groups of compounds present in gooseberry biomass.

### 4. Conclusions

In these studies, gooseberry (*Ribes uva-crispa* L.) waste obtained during processing in the food industry were tested for the possibility of Fe(III) ions biosorption in aqueous solutions. Firstly, several analytical methods were applied to determine the physicochemical properties of the biosorbent. Next, the effect of adsorbent dosage, initial concentration, pH, and contact time on the bioremoval efficiency was examined. According to the research results, the maximum adsorption efficiency of 88.5% (biomass dosage 100 g/L, pH 3, initial $C_0 = 10.7$ mg/L) and the calculated maximum

Table 3
Adsorption rate constants, $q_e$ and correlation coefficients associated with pseudo-first-order and the pseudo-second-order rate equations

| Adsorbent dosage (g/L) | Pseudo-first-order kinetic model | | | Pseudo-second-order kinetic model | | |
|---|---|---|---|---|---|---|
| | $k_{ad}$ (1/min) | $q_e$ (mg/g) | $R^2$ | $K$ (g/mg min) | $q_e$ (mg/g) | $R^2$ |
| 50 | 0.0118 | 0.174 | 0.374 | 0.201 | 4.882 | 0.921 |

Table 4
Isotherm model constants and correlation coefficients for biosorption of Fe(III) onto gooseberry

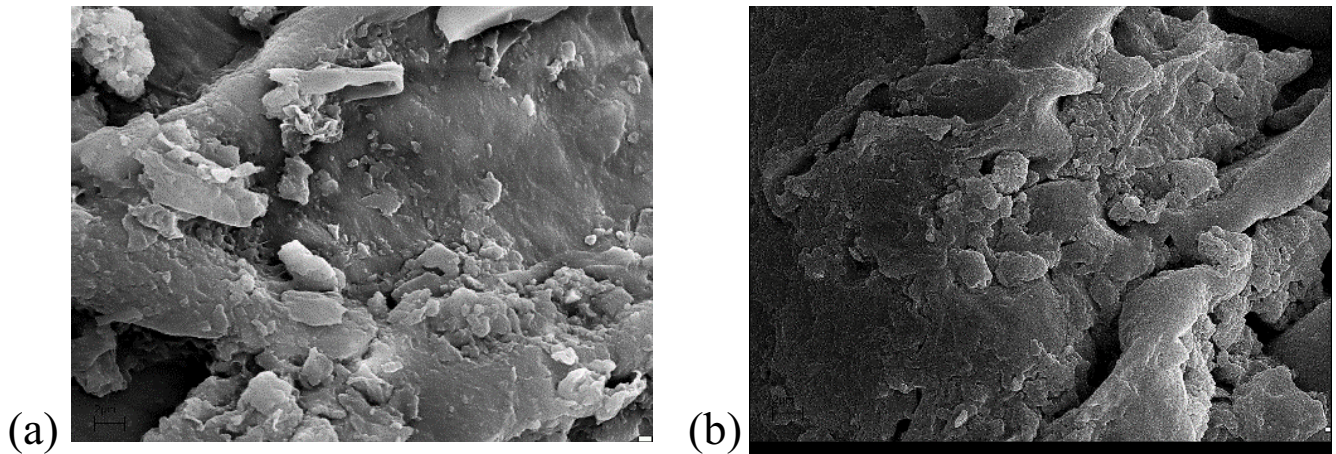| Adsorbent dosage (g/L) | Langmuir isotherm | | | Freundlich isotherm | | |
|---|---|---|---|---|---|---|
| | Calculated $q_m$ (mg/g) | $K_L$ (L/mg) | $R^2$ | $K_F$ (mg/g) (L/mg)$^{(1/n)}$ | $n$ | $R^2$ |
| 1 | 1.337 | 0.734 | 0.966 | 0.847 | 1.008 | 0.961 |

Fig. 7. (a and b) SEM images of gooseberry (×10,000) before (a) and after (b) Fe(III) biosorption.
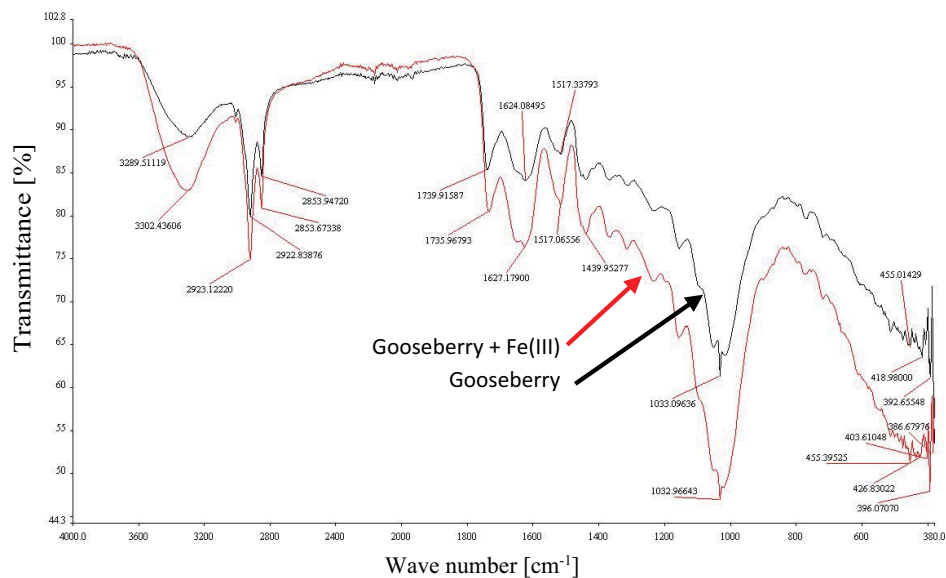


Fig. 8. FT-IR spectrum of gooseberry before and after Fe(III) ions biosorption.

Table 5
A comparison of adsorption capacity of Fe(III) ions onto various adsorbents

| Type of adsorbent/reference | $q_m$ (mg/g) |
| --- | --- |
| Gooseberry *Ribes uva-crispa* (these studies) | 1.337 |
| The husk of *Cicer arientinum* [28] | 72.16 |
| *Brown algae Sargassum Vulgare* [22] | 63.67 |
| Olive Cake [29] | 58.479 |
| Padina sanctae crucis algae [31] | 34.65 |
| Pretreated orange peel [32] | 18.19 |
| Oil palm frond [30] | 17.986 |
| Oil palm bark [30] | 16.207 |
| Hazelnut hull [33] | 13.59 |
| Empty fruit bunch [30] | 1.33 |
| Oil palm leaves [30] | 1.131 |

adsorption capacity of 1.34 mg/g were obtained. Finally, the process kinetics was carried out, isotherms were determined and characteristic parameters were calculated and analyzed. It should be noted that this biosorption process is better described by the pseudo-second-order kinetic model and the Langmuir model.

To sum up, the research has shown that gooseberry waste effectively removes Fe(III) ions from aqueous solutions due to the content of appropriate functional groups in its composition and favorable physical and chemical properties. The success obtained in the research can certainly be a new guideline to the use of this biomass to improve fresh water quality.

**Acknowledgment**

Table 6
FT-IR peaks of gooseberry and their assignment

| FT-IR band (cm$^{-1}$) | Assignment (vibrations, species) |
|---|---|
| 3,302; 3,289 | Stretching O–H from water and other hydroxylated molecules (alcohols, phenols) |
| 2,923 | Asymmetric stretching C–H, –CH$_3$, and –CH$_2$– groups (carboxylic acids) |
| 2,854 | Stretching C–H, –CH$_3$ groups |
| 1,736, 1,740 | Stretching C=O (esters) |
| 1,627, 1,624 | Stretching C–O |
| 1,517 | Bending N–H; stretching C=C (aromatic ring) |
| 1,440 | Bending O–H, bending C–H (–CH$_2$ group from proteins) |
| 1,380 | Deformation vibration C–H |
| 1,300 | Deformation vibration C–O, O–H (poliphenols) |
| 1,230 | Stretching C–O–C |
| 1,150 | Deformation vibration C–H, C–O, bending C–C (carbohydrates) |
| 1,033 | Bending C–O (polysaccharides) |
| 723 | Bending C–H |
| 455, 426, 419, 404, 396, 393 | Bending Si–O–Si |

## References

[1] L. Baroni, L. Cenci, M. Tettamanti, M. Berati, Evaluating the environmental impact of various dietary patterns combined with different food production systems, Eur. J. Clin. Nutr., 61 (2007) 279–286.

[2] S.L.R.K. Kanamarlapudi, V.K. Chintalpudi, S. Muddada, Application of Biosorption for Removal of Heavy Metals from Wastewater, J. Derco, B. Vrana, Eds., Biosorption, Intechopen Publisher, London, 4 (2018) 69–116.

[3] T. Kalak, J. Dudczak, R. Cierpiszewski, Adsorption Behaviour of Copper Ions on Elderberry, Gooseberry and Paprika Waste from Aqueous Solutions, Proceedings of 12th International Interdisciplinary Meeting on Bioanalysis (CECE), Brno, Czech Republic, 2015, pp. 123–127.

[4] Factfish, 2017. Available at: http://www.factfish.com/statistic/gooseberries%2C%20production%20quantity (Accessed November 5, 2019).

[5] Agricultural Market Agency, Fruit Market in Poland, Report, 2014.

[6] K. Hempfling, K.-H. Engel, Analysis and sensory evaluation of gooseberry (*Ribes uva crispa* L.) volatiles, Flavour Sci., 22 (2014) 123–127.

[7] N. Das, P. Karthika, R. Vimala, V. Vinodhini, Use of natural products as biosorbent of heavy metals–an overview, Nat. Prod. Radiance, 7 (2008) 133–138.

[8] C. Shanthi, R. Kingsley Porpatham, N. Pappa, Image analysis for particle size distribution, Int. J. Eng. Technol., 6, (2014) 1340–1345.

[9] T. Kalak, A. Kłopotek, R. Cierpiszewski, Effective adsorption of lead ions using fly ash obtained in the novel circulating fluidized bed combustion technology, Microchem. J., 145 (2019) 1011–1025.

[10] W. Peng, Q. Wu, P. Tu, N. Zhao, Pyrolytic characteristics of microalgae as renewable energy source determined by thermogravimetric analysis, Bioresour. Technol., 80 (2001) 1–7.

[11] L.B. McCusker, IUPAC nomenclature for ordered microporous and mesoporous materials and its application to non-zeolite microporous mineral phases, Rev. Mineral. Geochem., 57 (2005) 1–16.

[12] D. Paliulis, J. Bubėnaitė, Effect of pH for Lead Removal from Polluted Water Applying Peat, The 9th International Conference on Environmental Engineering, Vilnius, Lithuania, 2014.

[13] H. Lata, V.K. Garg, R.K. Gupta, Sequestration of nickel from aqueous solution onto activated carbon prepared from *Parthenium hysterophorus* L., J. Hazard. Mater., 157 (2008) 503–509.

[14] Y. Nuhoglu, E. Malkoc, Thermodynamic and kinetic studies for environmentally friendly Ni(II) biosorption using pomace of olive oil factory, Bioresour. Technol., 100 (2009) 2375–2380.

[15] S. Benaisa, R. El Mail, N. Jbari, Biosorption of Fe(III) from aqueous solution using brown algae *Sargassum vulgare*, J. Mater. Environ. Sci., 7 (2016) 1461–1468.

[16] L. Nouri, I. Ghodbane, O. Hamdaoui, M. Chiha, Batch sorption dynamics and equilibrium for the removal of cadmium ions from aqueous phase using wheat bran, J. Hazard. Mater., 149 (2007) 115–125.

[17] R. Ovcharenko, E. Voloshina, J. Sauer, Water adsorption and O-defect formation on Fe$_2$O$_3$(0001) surfaces, Phys. Chem. Chem. Phys., 18 (2016) 25560–25568.

[18] V.P. Vinod, T.S. Anirudhan, Sorption of tannic acid on zirconium pillared clay, J. Chem. Technol. Biotechnol., 77 (2001) 92–101.

[19] T. Kalak, R. Cierpiszewski, Correlation analysis between particulate soil removal and surface properties of laundry detergent solutions, Text. Res. J., 85 (2015) 1884–1906.

[20] X. Li, Y. Tang, X. Ca, D. Lu, L. Fang, W. Shao, Preparation and evaluation of orange peel cellulose adsorbents for effective removal of cadmium, zinc, cobalt and nickel, Colloids Surf., A, 317 (2008) 512–521.

[21] N. Feng, X. Guo, S. Liang, Adsorption study of copper(II) by chemically modified orange peel, J. Hazard. Mater., 164 (2009) 1286–1292.

[22] J.C.P. Vaghetti, E.C. Lima, B. Royer, N.F. Cardoso, B. Martins, T. Calvete, Pecan nutshell as biosorbents to remove toxic metals from aqueous solution, Sep. Sci. Technol., 44 (2009) 615–644.

[23] P. Janos, J. Fedorovic, P. Stankova, S. Gröteschelová, J. Rejnek, P. Stopka, Iron humate as low-cost sorbent for metal ions, Environ. Technol., 27 (2006) 169–181.

[24] D. Kavitha, C. Namasivayam, Experimental and kinetic studies on methylene blue adsorption by coir pith carbon, Bioresour. Technol., 98 (2007) 14–21.

[25] W. Plazinski, J. Dziuba, W. Rudzinski, Modeling of sorption kinetics: the pseudo-second order equation and the sorbate intraparticle diffusivity, Adsorption, 19 (2013) 1055–1064.

[26] S.B. Wang, E. Ariyanto, Competitive adsorption of malachite green and Pb ions on natural zeolite, J. Colloid Interface Sci., 314 (2007) 25–31.

[27] P.S. Kumar, C. Vincent, K. Kirthika, K.S. Kumar, Kinetics and equilibrium studies of Pb$^{2+}$ ion removal from aqueous solutions by use of nano-silversol-coated activated carbon, Braz. J. Chem. Eng., 27 (2010) 339–346.

[28] N. Ahalya, R.D. Kanamadi, T.V. Ramachandra, Biosorption of iron(III) from aqueous solutions using the husk of *Cicer arientinum*, Indian J. Chem. Technol., 13 (2006) 122–127.

[29] Z.A. Al-Anber, M.A.S. Al-Anber, Thermodynamics and kinetic studies of iron(III) adsorption by olive cake in a batch system, J. Mex. Chem. Soc., 52 (2008) 108–115.

[30] S. Khosravihaftkhany, N. Morad, T.T. Teng, A.Z. Abdullah, I. Norli, Biosorption of Pb(II) and Fe(III) from aqueous solutions using oil palm biomasses as adsorbents, Water Air Soil Pollut., 224 (2013) 1455, doi: 10.1007/s11270-013-1455-y.

[31] M. Keshtkar, S. Dobaradaran, S. Akbarzadeh, M. Bahreini, D.R. Abadi, S.G. Nasab, F. Soleimani, N. Khajeahmadi, M.M. Baghmolaei, Iron biosorption from aqueous solution by *Padina sanctae* crucis algae: isotherm, kinetic and modelling, Int. J. Pharm. Technol., 8 (2016) 10459–10471.

[32] V. Lugo-Lugo, C. Barrera-Díaz, F. Ureña-Núñez, B. Bilyeu, I. Linares-Hernández, Biosorption of Cr(III) and Fe(III) in single and binary systems onto pretreated orange peel, J. Environ. Manage., 112 (2012) 120–127.

[33] A. Sheibani, M.R. Shishehbor, H. Alaei, Removal of Fe(III) ions from aqueous solution by hazelnut hull as an adsorbent, Int. J. Ind. Chem., 3 (2012) 1–4.